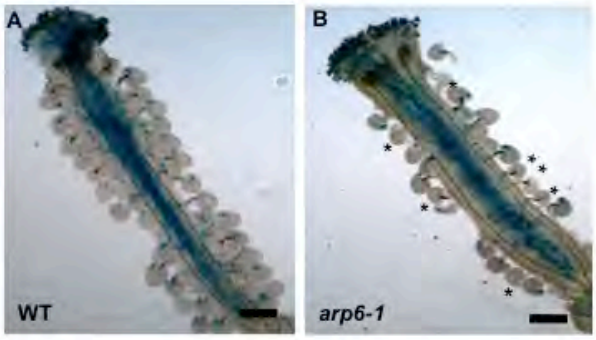

C

Plant genotype*	Targeted ovules (%)	Untargeted ovules (%)
+/+	407 (88.86)	51 (11.14)
arp6-1	218 (53.56)	139 (46.44)

**pLAT52:GUS* pollen was pollinated onto pistils from indicated genotypes

D

Pistil	Ovules	# of available ovules	# of targeted ovules	Targeting efficiency (%)	Least squares-mean
+/+	+/+	206	112	54.37	65.3[a]
arp6-1	+/+	203	107	52.71	62.6[a]
arp6-1	*arp6-1*	189	59	31.22	27.7[b]
+/+	*arp6-1*	212	71	33.49	35.3[b]

Supplemental Figure 1. Reproductive defects in *arp6-1* pistils.

(A) A wild-type (WT) pistil pollinated with *pLAT52:GUS* pollen.

(B) An *arp6-1* pistil pollinated with *pLAT52:GUS* pollen. Ovules not targeted by a pollen tube are indicated with black asterisks (*). Note that the pollen tube growth in the transmitting tract in an *arp6-1* pistil is comparable to WT.

Scale bars (A) and (B) = 100 μm.

(C) Quantification of defects in pollen tube targeting to WT and *arp6-1* ovules in pistils.

(D) Quantification of defects in pollen tube targeting to WT and *arp6-1* ovules in a semi *in vivo* pollen tube targeting assay.

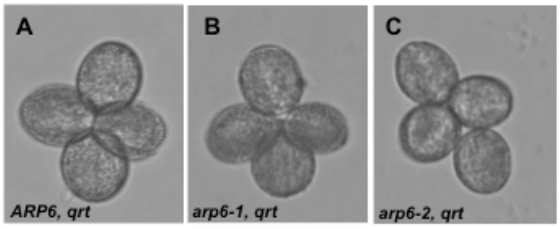

D

Plant genotype*	Tetrad with four normal pollen (%)	Tetrad with ≥1 defective pollen (%)	n
+/+	505 (97.49)	13 (2.51)	6
arp6-1	595 (96.43)	22 (3.57)	7
arp6-2	532 (96.03)	22 (3.97)	7

*All plants carry *qrt/qrt* mutation; n, number of plants observed

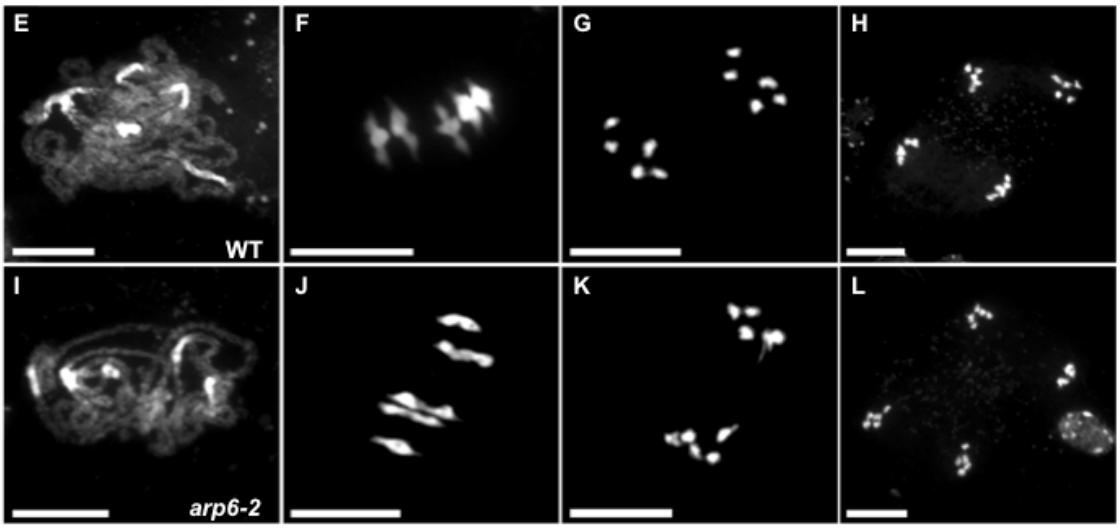

Supplemental Figure 2. Analysis of meiotic divisions of microsporogenesis.

(A-D) Pollen development is apparently normal in *arp6* mutants. Wild-type (WT) (A), *arp6-1* (B), and *arp6-2* (C) pollen tetrads in *qrt* background did not exhibit pollen developmental defects. (D) Table showing enumeration of apparently normal pollen tetrads in wild-type and *arp6* mutants.

(E-L) Meiosis during microsporogenesis is apparently normal in *arp6* mutants. (E) and (I) WT and *arp6-2* microsporocytes, respectively, at pachytene stage of prophase I showing apparently normal synapsis of homologous chromosomes.

(F) and (J) WT and *arp6-2* microsporocytes, respectively, at metaphase I stage showing five bivalents alignment aligned at the equator.

(G) and (K) WT and *arp6-2* microsporocytes, respectively, at the anaphase I stage showing non-random segregation of the ten homologous chromosomes.

(H) and (L) WT and *arp6-1* microsporocytes, respectively, at anaphase II showing non-random segregation of sister chromatids.

(E-L) Scale bars = 10 μm

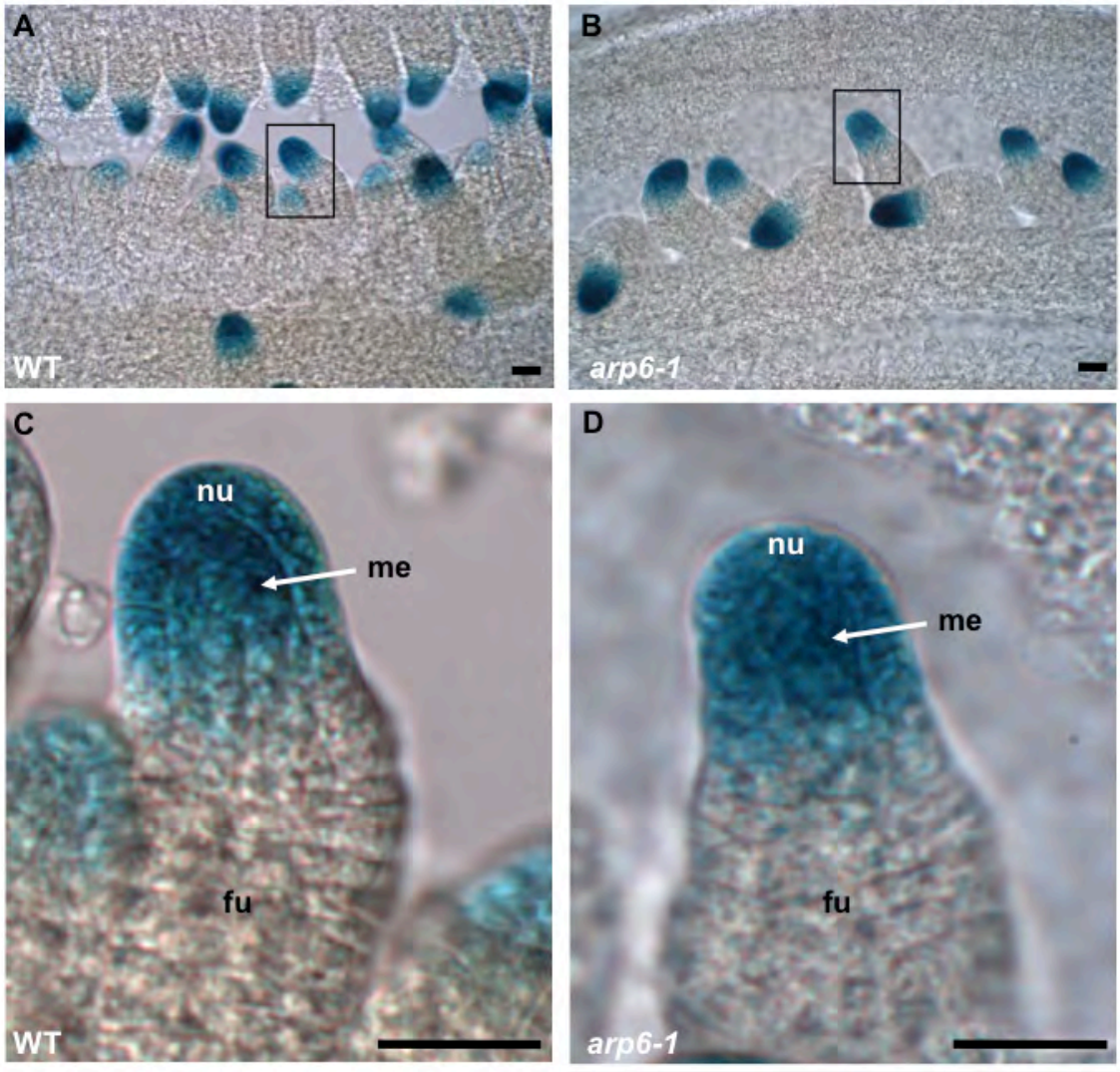

Supplemental Figure 3. *pSPL:GUS* expression in *arp6-1* ovules is comparable to wild type.

(A) GUS expression in wild-type (WT) stage 2-I ovules (prior to entering meiosis) carrying *pSPL:GUS* (390/390, n=6 pistils).

(B) GUS expression in *arp6-1* stage 2-I ovules carrying *pSPL:GUS* (334/334, n=8 pistils).

(C) and (D) Close-up views of ovules marked by black squares in (A) and (B) respectively, showing *pSPL:GUS* expression in the megasporocyte (me) and distal nucellus (nu) but not in the developing funiculus (fu) of stage 2-I ovules.

(A-D) Scale bars = 10 μm.

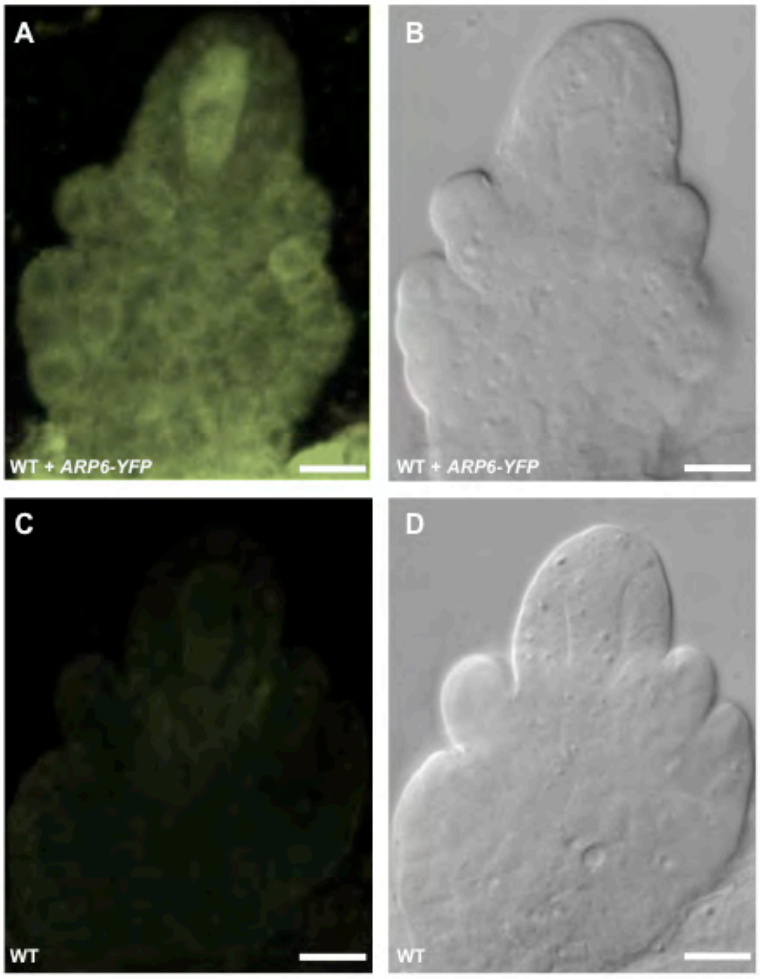

Supplemental Figure 4. Localization of ARP6-YFP fusion protein in ovules undergoing megasporogenesis.

(A) Confocal Laser Scanning Microscopy (CLSM) image showing ARP6-YFP fusion protein activity in a stage 2-III/IV wild-type (WT) ovule carrying *ARP6-YFP* transgene. Image shown is a projection of six optical sections spanning ~60 μm.

(B) Bright field image of the ovule shown in (A).

(C) CLSM image of a stage 2-III/IV ovule from a non-transformed WT plant.

(D) Bright field image of the WT ovule shown in (C).

(A) and (C) CLSM images were captured using identical image acquisition settings.

(A-D) Scale bars = 4 μm.

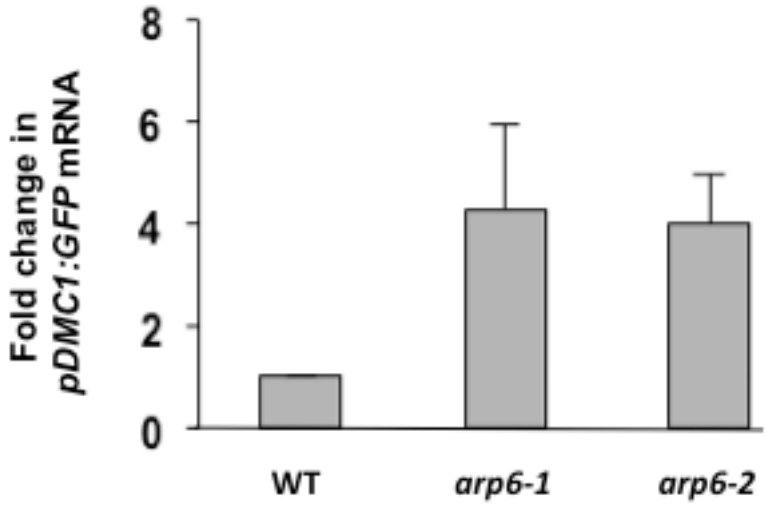

Supplemental Figure 5. RT-qPCR analysis of *GFP* expression levels in wild-type, *arp6-1*, and *arp6-2* stage 2-III/IV ovules carrying *pDMC1:GFP*. Graph shows fold change in GFP mRNA levels in each genotype as compared to the levels in wild-type ovules based on an average of two biological replicates normalized to ACTIN2/8 mRNA levels. Error bars in the graph refer to the standard deviation of the data.

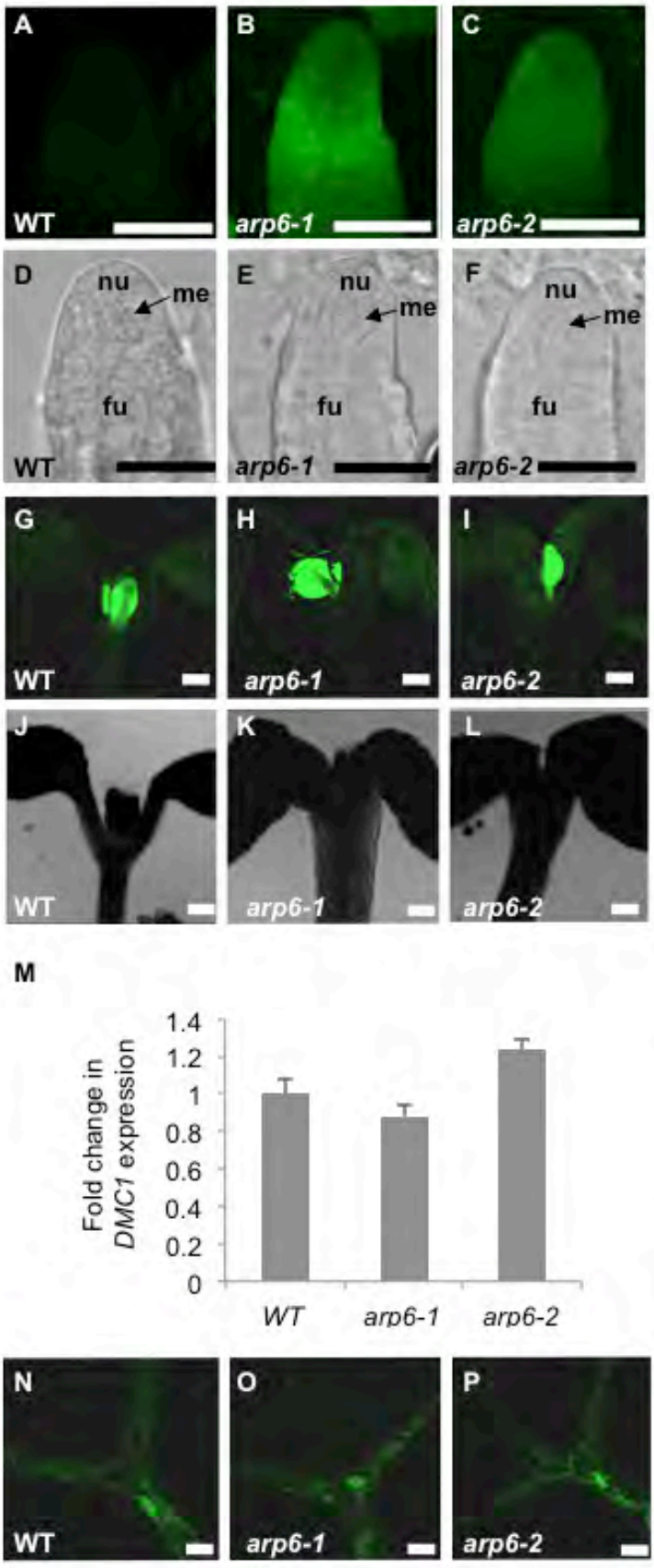
A
B
C
WT
arp6-1
arp6-2
D
E
F
nu
me
fu
WT
arp6-1
arp6-2
G
H
I
WT
arp6-1
arp6-2
J
K
L
WT
arp6-1
arp6-2
M
Fold change in DMC1 expression
1.4
1.2
1
0.8
0.6
0.4
0.2
0
WT
arp6-1
arp6-2
N
O
P
WT
arp6-1
arp6-2

Supplemental Figure 6. Analysis of *pDMC1:GFP* expression during ovule and seedling development in wild-type and *arp6* plants.

(A) Confocal Laser Scanning Microscopy (CLSM) image of *pDMC1:GFP* expression in stage 2-I wild-type (WT) ovule.

(B) CLSM image of *pDMC1:GFP* expression in stage 2-I *arp6-1* ovule.

(C) CLSM image of *pDMC1:GFP* expression is detected in stage 2-I *arp6-2* ovule.

(D-F) Bright-field image of (A), (B), and (C), respectively.

(A-F) me, megasporocyte; fu, funiculus; nu, nucellus. Scale bars = 20 μm.

(G-P) Ectopic expression of *pDMC1:GFP* is not detected in *arp6* vegetative tissues. (G) CLSM image of *pDMC1:GFP* expression in true leaves in a five-day old Wild-type (WT) seedling.

(H) CLSM image of *pDMC1:GFP* expression in true leaves in a five-day old *arp6-1* seedling.

(I) CLSM image of *pDMC1:GFP* expression in true leaves in a five-day old *arp6-2* seedling.

(J-L) Bright-field images of (G), (H), and (I), respectively.

(M) RT-qPCR analysis of endogenous *DMC1* expression levels in WT, *arp6-1*, and *arp6-2* seedlings. Results shown in the graph is the fold change in *DMC1* expression in *arp6* mutants compared to that in wild type. Results are an average of three biological replicates of *DMC1* expression normalized to expression of *HK2* in each genotype.

(N) CLSM image of *pDMC1:GFP* expression in cytoplasm and nucleus of a WT leaf trichome.

(O) CLSM image of *pDMC1:GFP* expression is observed in an *arp6-1* leaf trichome.

(P) CLSM image of *pDMC1:GFP* expression is observed in an *arp6-2* leaf trichome.

Scale bars (G-L) = 200 μm; (N-P) = 20 μm

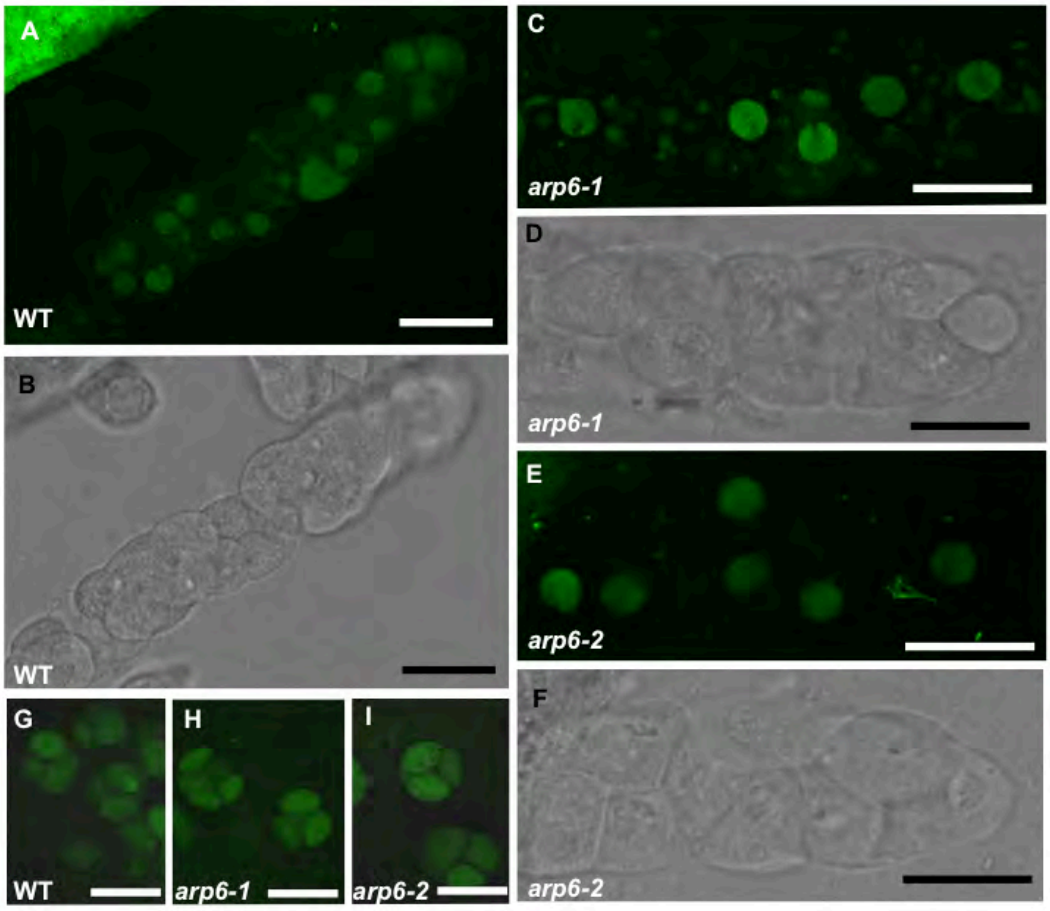

J

Plant genotype	GFP⁺ PMC	GFP⁻ PMC
WT	149 (55.19%)	121 (44.81%)
arp6-1	79 (51.97%)	71 (48.03%)
arp6-2	81 (54.00%)	69 (46.00%)

GFP⁺PMC, *DMC1:GFP*-positive pollen mother cells; GFP⁻PMC, *DMC1:GFP*-negative in pollen mother cells.

Supplemental Figure 7. *pDMC1:GFP* expression during meiosis of microsporogenesis remains apparently unaltered in *arp6* mutants.

(A-F) Confocal Laser Scanning Microscopy (CLSM) image (A, C, and E) or bright field images (B, D, and E) of wild-type (WT), *arp6-1*, and *arp6-2* microsporocytes.

(G-I) CLSM images of WT, *arp6-1*, and *arp6-2* pollen tetrads.

(J) Table showing enumeration of *pDMC1:GFP* expression in WT, *arp6-1*, and *arp6-2* microsporocytes.

(A-F) Scale bars = 20 μm.

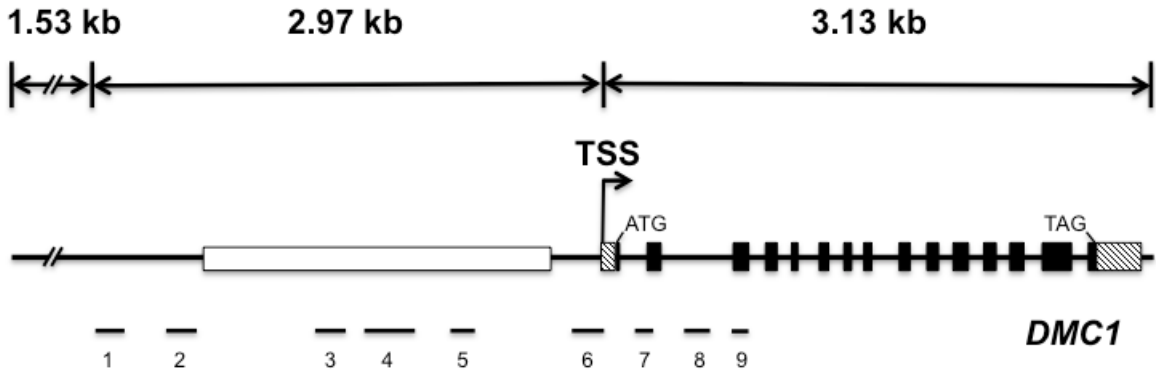

Supplemental Figure 8. *DMC1* gene structure in Arabidopsis (Col-0 ecotype). The diagram shows locations of PCR products (1-9) in *DMC1* assayed for H2A.Z deposition by ChIP-qPCR. Numbers 1-9 shown here also correspond to the numbers in the X-axis of graphs in Table 3 and Supplementary Figure 9. The promoter region shown includes the 1874 bp transposon insertion (white rectangle). TSS, transcription start site; black rectangles refer to the exons in *DMC1* and hatched boxes are 5' and 3' UTRs in *DMC1*.

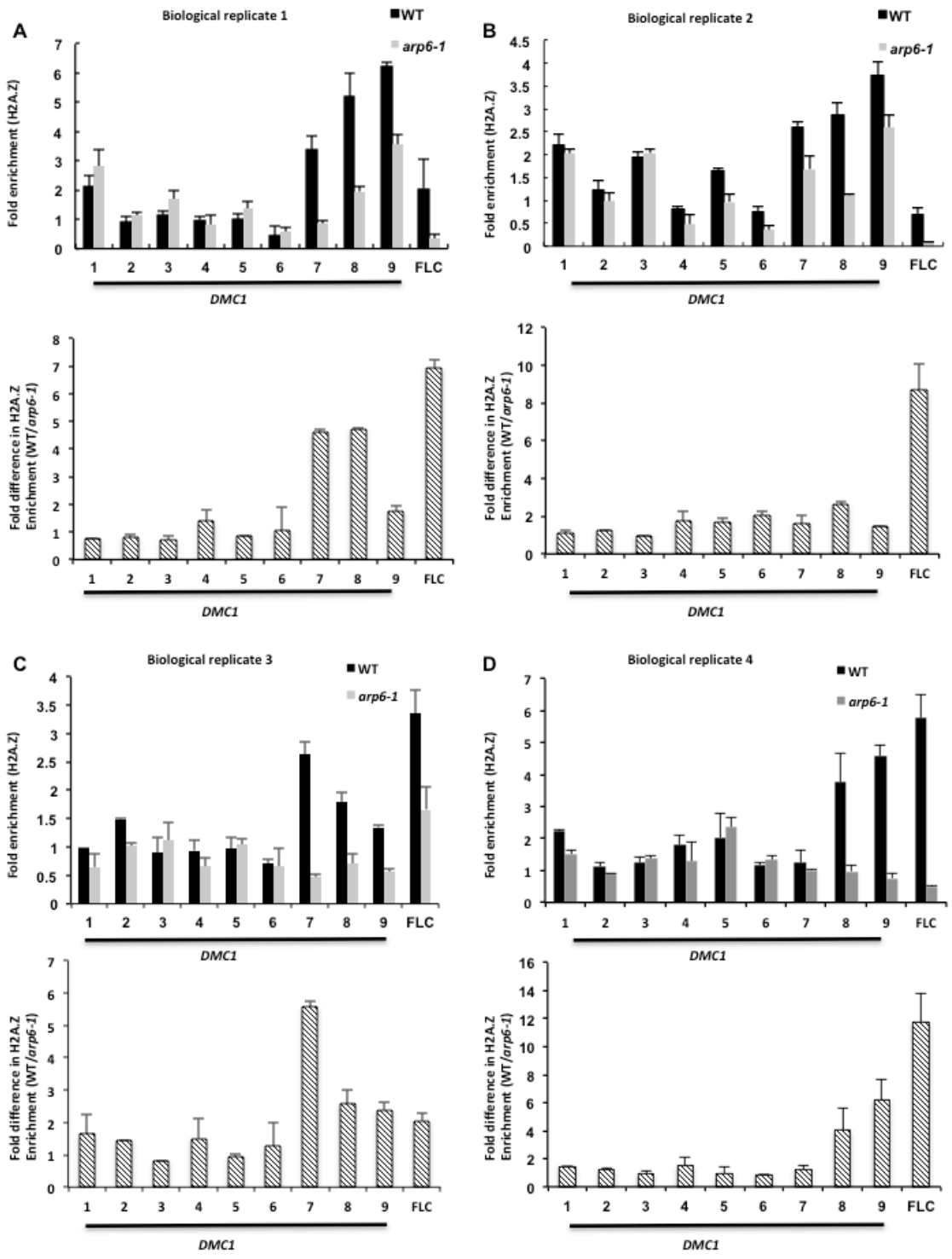
A
Biological replicate 1
WT
arp6-1
Fold enrichment (H2A.Z)
1 2 3 4 5 6 7 8 9 FLC
DMC1
Fold difference in H2A.Z Enrichment (WT/arp6-1)
B
Biological replicate 2
C
Biological replicate 3
D
Biological replicate 4

Supplemental Figure 9. H2A.Z deposition at the *DMC1* gene body is partially dependent on ARP6.

(A-D) ChIP-qPCR analysis of H2A.Z deposition in biological replicates 1 (A), 2 (B), 3 (C), and 4 (D). In each panel, the top graph shows the fold enrichment of H2A.Z deposition at indicated location of *DMC1* (1-9) and *FLOWERING LOCUS C* (*FLC*) in wild-type (WT) or *arp6-1* plants ± standard deviation of relative quantity values determined by ChIP-qPCR. The bottom graph in each panel shows fold difference in H2A.Z enrichment between wild type and *arp6-1* at indicated location ± standard deviation of relative quantity values reported in the corresponding top graph of that panel.

Supplemental Table 1. Confocal laser scanning microscopy observations of WT and *arp6-1* ovules

Ovule genotype	Normal FG* (%)	Abnormal FG^{+}(%)
+/+	80 (100)	0 (0)
arp6-1	51 (56.04)	40 (43.96)

FG, mature female gametophyte at stage FG7
*mature female gametophyte with four nuclei in the micropylar end
$^{+}$ovule with no female gametophyte

Supplemental Table 1. Quantification of confocal laser scanning microscopy observations of WT and *arp6-1* ovules at mature female gametophyte stage (FG7) reported in Figure 1A-D.

Supplemental Table 2. Confocal laser scanning microscopy observations of megagametogenesis

Ovule genotype	Normal FG* (%)	Abnormal FG^{+}(%)
+/+	104 (100)	0 (0)
arp6-1	92 (56.04)	69 (43.96)

FG, female gametophyte undergoing megagametogenesis
*female gametophyte with 1-2 nuclei
$^{+}$female gametophyte with no degenerating megaspore or functional megaspore

Supplemental Table 2. Quantification of confocal laser scanning microscopy observations of megagametogenesis reported in Figure 1I-Q

Supplemental Table 3. Reduced fertility in *arp6-1* and *arp6-2* mutants is caused by defects in sporophytic tissues in pistils

Female parent	Male parent	Normal seeds (%)		Aborted seeds (%)		Unfertilized ovules (%)	
arp6-1/+	*+/+*	810	(97.0)	0	(0.0)	25	(3.0)
+/+	*arp6-1/+*	979	(96.3)	2	(0.2)	36	(3.5)
arp6-2/+	*+/+*	606	(99.2)	0	(0.0)	5	(0.8)
+/+	*arp6-2/+*	863	(97.7)	1	(0.1)	19	(2.2)
+/+	*+/+*	683	(95.4)	2	(0.3)	31	(4.3)
arp6-1	*+/+*	415	(60.5)	3	(0.4)	268	(39.1)
+/+	*arp6-1*	997	(97.2)	1	(0.1)	28	(2.7)
arp6-2	*+/+*	1538	(76.0)	4	(0.2)	481	(23.8)
+/+	*arp6-2*	782	(96.3)	1	(0.1)	29	(3.6)

Supplemental Table 3. Reciprocal crosses between wild-type and *arp6* heterozygotes or homozygotes were performed. Crossed siliques were opened 10 days after pollination and number of viable seeds, aborted seeds, and unfertilized ovules were counted. The crosses exhibited reduced fertility only when *arp6* plants were used as female parents, indicating that the reduced fertility phenotype is determined by the lack of *ARP6* function in the sporophyte rather than in the female gametophyte.

Supplemental Table 4. Meiosis during megasporogenesis is abnormal in *arp6* megasporocytes

	Dyad	Triad1 (%)	Tetrad1 (%)	Tetrad2 (%)	Tetrad3 (%)	Triad2 (%)	Abnormal (%)	Total
+/+	17 (8.72)	46 (23.59)	92 (47.18)	24 (12.31)	16 (8.21)	0 (0)	0 (0)	195
arp6-1	25 (9.77)	122 (47.66)	3 (1.17)	0 (0)	0 (0)	42 (16.40)	64 (25.00)	256
arp6-2	23 (11.33)	84 (41.38)	2 (0.99)	0 (0)	0 (0)	66 (32.51)	28 (13.79)	203

Supplemental Table 4. Callose-stained ovules from either wild type or *arp6* inflorescences were observed for meiosis progression. The indicated meiosis stages in megasporocytes are as shown in Figure 2. Numbers within parentheses refer to the % meiosis stage type within an inflorescence of indicated genotypes.

Supplemental Table 5. Expression of meiosis-related genes in *arp6* anthers

Gene	*arp6-1/WT*			*arp6-2/WT*		
	LSM [#]	Std. Dev.	*P* value	LSM [#]	Std. Dev.	*P* value
DMC1	1.17 [b]	0.29	0.27	1.39 [b]	0.31	0.09
ASY1	2.04 [b]	0.81	0.09	2.12 [b]	1.89	0.38
DYAD	1.18 [b]	0.27	0.22	0.99 [b]	0.25	0.84
MND1	1.20 [b]	0.26	0.18	1.28 [b]	0.35	0.22
AML4	0.97 [b]	0.27	0.88	1.39 [b]	0.32	0.09
SPO11	1.28 [b]	0.64	0.43	1.59 [b]	0.25	0.02*
DIF1	1.96 [b]	0.99	0.17	1.32 [b]	0.47	0.28
ATM	1.42 [b]	0.27	0.05*	1.60 [b]	0.59	0.15
SDS	1.23 [b]	0.48	0.04*	0.85 [b]	0.46	0.71
AML1	2.42 [b]	1.73	0.24	2.33 [b]	2.39	0.40
RAD51	1.63 [b]	0.72	0.19	1.38 [b]	0.51	0.26
SAP	6.55 [a]	2.17	0.01*	9.87 [a]	2.88	0.01*
SPL	1.42 [b]	0.34	0.08	1.24 [b]	0.32	0.23

LSM, Least-Squares Mean of change in expression of a meiosis-related gene in *arp6-1* or *arp6-2* compared to that in wild-type (WT) anthers in five technical replicates (three biological replicates) assayed by RT-qPCR.
Std. Dev., standard deviation.
P value, probability value associated with a pairwise test between change in the expression of a gene in *arp6-1* or *arp6-2* compared to that in WT anthers and change in the expression of *ACTIN2* in *arp6-1* or *arp6-2* compared to that in WT anthers. * $P \leq 0.05$.
[#]Any pair of LSMs that do not share the same letter are significantly different ($P \leq 0.05$) from each other in pairwise comparisons for change in expression of a meiosis-related gene in *arp6-1* or *arp6-2* compared to that in wild-type (WT) anthers.

Supplemental Table 6. *pDMC1:GFP* expression is affected in *arp6* megasporocytes

Plant genotype	GFP-positive megasporocytes (%)	GFP-negative megasporocytes (%)	Total*
+/+	270 (93.43)	19 (7.57)	289
arp6-1	157 (52.86)	140 (47.14)	290
arp6-2	150 (66.97)	74 (33.03)	224

Supplemental Table 6. Quantification of confocal laser scanning microscopy observations of *pDMC1:GFP* expression in ovules reported in Figures 5D to 5H. The frequency of ovules with GFP staining in the megasporocyte (GFP-positive) or without GFP staining in the megasporocyte (GFP-negative) are shown in the table. *Total number of megasporocytes observed.

Supplemental Table 7. List of primers used in this study

Gene	Name	Primer sequence	Product size (bp)	Used in
At5g35770	SAPF1 SAPR1	TCTTCTTCTTCCCCTGTTCCTC TTGGCGAGATAGTAGTTGCCAT	311	RT-qPCR (Table 2)
At3g33520	ARP6F1 ARP6R1	ACCACTTACAGAGTTCGTTCGC GAAAGAATCGTCTACGACACCG	1308	RT-PCR (Table 2)
At5g61960	AML1F1 AML1R1	TCCACATAGGTTCTCATGGTAG CGTTCATTAAGCTTGAGTTCTG	630	RT-qPCR (Table 2)
At5g07290	AML4F1 AML4R1	ATGGATTTTGGTTCTCATAAGG TCAAACTTGAGTTCTGGAAATG	571	RT-qPCR (Table 2)
At5g20850	RAD51F1 RAD51R1	TACAGATAGCTGACAGGTTTGG ACTTACAAAGCTCTTTTGCTCC	678	RT-qPCR (Table 2)
At1g63990	SPO11F1 SPO11R1	GAAAAGCATGCGATCTTTCATC CCAGTTTGAACCATCAGTGACA	410	RT-qPCR (Table 2)
At5g51330	DYADF1 DYADR1	GGAGAAATCCGTGACATCAGAG TGTTGATCATGCTTCCTTCCTT	431	RT-qPCR (Table 2)
At3g48190	ATMFP1 ATMRP1	CATTACTTCGCAAGGGAACAAG GATGAAACCAAGTTTGGCTCTG	378	RT-qPCR (Table 2)
At1g14750	SDSFP1 SDSRP1	AATGCTTCACACCCACAATCTT AACCTGTGTGTTGGTATCGGAG	352	RT-qPCR (Table 2)
At1g67370	ASY1F1 ASY1R1	CATGGTGGAGCTGTTAAGGAAG TCTTCCCAAAAGTGCGATAAGA	306	RT-qPCR (Table 2)
At4g29170	MND1F1 MND1R1	TAGCAGTGTTTGAAATCCTTTG AATCAAAGTCCTCAGTGATTCC	664	RT-qPCR (Table 2)
At5g05490	DIF1F1 DIF1R1	CTAAAAGTCGCATGCCCAATAG ATGAGAATGTCCCCATAAGGCT	406	RT-qPCR (Table 2)
At3g22880	DMC1-0F DMC1-0R	TAGGATTCTGATTGTTGACTCG TTTTACAAACGAACCAGAGTTG	582	RT-qPCR (Table 2)
S65T	SGFPF1 SGFPR1	ATGGTGAGCAAGGGCGAGGAGC GTACAGCTCGTCCATGCCGTGA	729	*pDMC1:GFP* (Figure 5)
At3g18780	ACTIN2F1 ACTIN2R1	CCTATTGAGCATGGTGTTGTTAGCAC TGTGAGACACACCATCACCAGA	277	RT-PCR (Table 2)
At3g18780	ACTIN2F2 ACTIN2R2	TCCCTCAGCACATTCCAGCAGAT AACGATTCCTGGACCTGCCTCATC	68	RT-qPCR (Figure S7)
At4g26410	HK2F HK2R	GATTGGTGTCGCTGCTAGTCTC AGAATTGTGCCTCTTCGCTCTG	98	RT-qPCR (Figure S7)
At3g22880	DMC1 2.7 5' *SalI* DMC1 3' *BglII*	ACGTGTCGACACACCTAATCGGTGA TTGCC GCAGATCTAGCCATCATTTTCTCGCT CTAAGAC	2700	*pDMC1:GFP* (Figure 5)
At3g22880	DMC1-1F DMC1-1R	CCACATATACCTTTACACTAGAG GCACTTCACAACTCATATATTG	172	ChIP-qPCR (Table 3)
At3g22880	DMC1-2F DMC1-2R	CGACATTGGGACTCCTCACTAC TCTACCAACTATCATATTATCC	172	ChIP-qPCR (Table 3)
At3g22880	DMC1-3F DMC1-3R	GAGATGTTGAAAATCGTTTCTC CATGGAAAGAAATCACAAACCTG	175	ChIP-qPCR (Table 3)
At3g22880	DMC1-4F DMC1-4R	AATCAAGTTGGGAATCAATAGG CGCCGTAAGAGCTACAAACAC	289	ChIP-qPCR (Table 3)
At3g22880	DMC1-5F DMC1-5R	ATGCGGTTGATTTGCTAC CACGGTTAATCGAATCTCCT	141	ChIP-qPCR (Table 3)

At3g22880	DMC1-6F DMC1-6R	ACGGATGATAACTATGACG TTTGCTCGATTTGCTTCGAGGGTTC	187	ChIP-qPCR (Table 3)
At3g22880	DMC1-7F DMC1-7R	TGTACCTGACTCGCTTCTTCTCGT AGCTGCATCTGGCTCGTTTCTTCA	105	ChIP-qPCR (Table 3)
At3g22880	DMC1-8F DMC1-8R	CTCGTTGTTGCTTAATCGCTGGGT CGTTACCAAGGAGAACCATGTTCAG	152	ChIP-qPCR (Table 3)
At3g22880	DMC1-9F DMC1-9R	CTTGTGTCAGTGATCGCACAAGGT GGTATGCATCATGAGACCATTGCAGG	96	ChIP-qPCR (Table 3)
At5g10140	FLC-F FLC-R	AAAGTAGCCGACAAGTCA AAACCCAGGTAAGGAAAA	170	ChIP-qPCR (Table 3)
At3g22880	DMC1-probe-F DMC1-probe-R	TTAGGTCTGGGAAAACCCAATTAG AGTTCTCCTCTTCCAGTGAAATCC	328	In situ Hybridization (Figure 5)
At3g33520	ARP6 probe-F ARP6 probe-R	CAAAGGCTATGTTAAAGACCCTCA GTCGAAGCTCTCCTTCTAGTCTCT	335	In situ Hybridization (Figure 4)
At3g33520	ARP6 5' Kpn2 ARP6 3' Sac1	ACGTGGTACCCACACTCATTTGGATT GACACC ACGTGAGCTCGTGCAACAGCCTGAT ACAGTAGC	5400	Complementation of *arp6* mutant phenotypes

Supplemental Table 7. List of primer pair names, sequences, and the expected size of PCR products are shown.

Supplemental Table 8. Identification of transgenic plants expressing *pDMC1:GFP*

T1 Plant #	GFP Expression in ovules or megasporocyte (MMC), floral buds, and stamens	% Kan^R T2 plants	T2 plants showing MMC expression (positives/total tested)	T2 plant used in crosses to *arp6* mutants
1	ovules (+), immature buds (+)	-	-	-
2	ovules (+/-)	-	-	-
3	ovules (+), buds (+), stamens (+)	-	-	-
4	ovules (++), MMC (-)	-	-	-
5	MMC (+/-), integuments	-	-	-
6	ovules (+/-)	-	-	-
7	all organs tested (+/-)	-	-	-
8	buds (++),carpel wall (?), stamens (++)	-	-	-
9	MMC (+),integuments (+), buds (+)	95.8		
10	MMC (-), buds (-), stamens (-)	-	-	-
11	MMC (+/-), buds (-)	-	-	-
12	MMC (+/-), buds (+/-), stamens (+/-)	-	-	-
13	MMC (+),integuments (?), buds (+)	87.2	4/4	#13-4
14	MMC (+/-), buds (+/-)	92.1	-	-
15	MMC (+), buds (-)	71.4	3/3	-
16	MMC (+), later integuments (+), buds (+), stamens (+)	86.2	0/4	-
17	MMC (-), buds (+/-)	-	-	-
18	MMC (+), buds (+)	100.0	-	-